Supporting Information

Ruthenium Nanoframe/ Enzyme Composite System as a Self-Activating Cascade Agent for the Treatment of Bacterial Infections

Dongliang Huo, Zhi Jia, Yanan Liu, Xufeng Zhu, Xu Chen, Ange Lin, Jie Liu*

Address：Department of Chemistry, College of Chemistry and Materials Science, Jinan University, Guangzhou 511436, China.

E-mail: tliuliu@jnu.edu.cn.*Corresponding author.

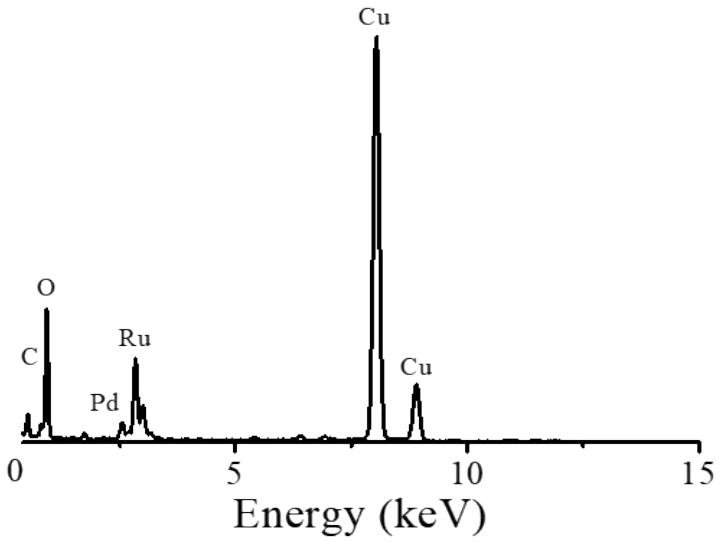

Figure. S1. EDS spectrum of Ru NFs.

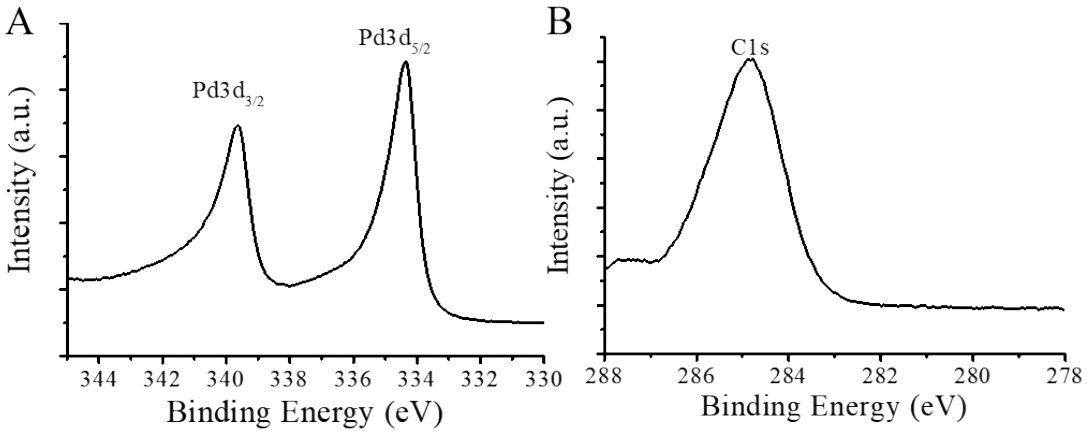

Figure. S2. (A) and (B) XPS spectra of Pd NPs.

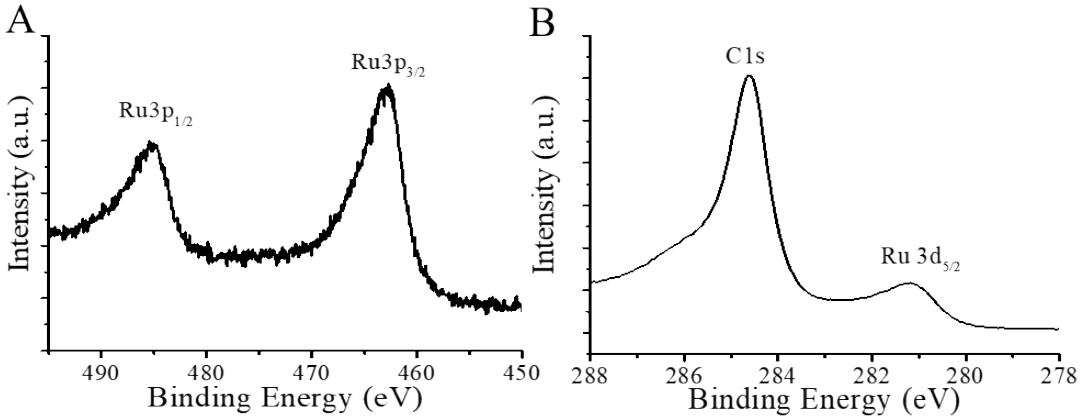

Figure. S3. (A) and (B) XPS spectra of Ru NFs.

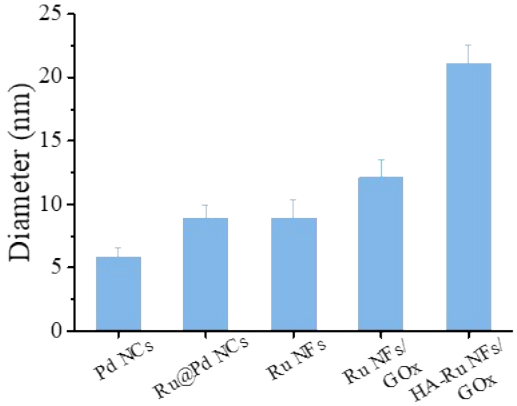

Figure. S4. Size distributions of Pd NPs, Ru-Pd NPs, Ru NFs, Ru NFs/GOx and HA-Ru NFs/GOx during the synthesis process.

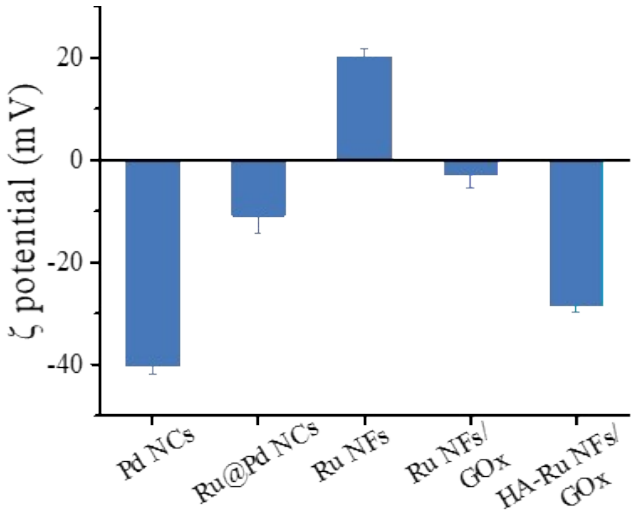

Figure. S5. Variation of ζ-potentials of Pd NPs, Ru-Pd NPs, Ru NFs, Ru NFs/GOx and HA-Ru NFs/GOx during the synthesis process.

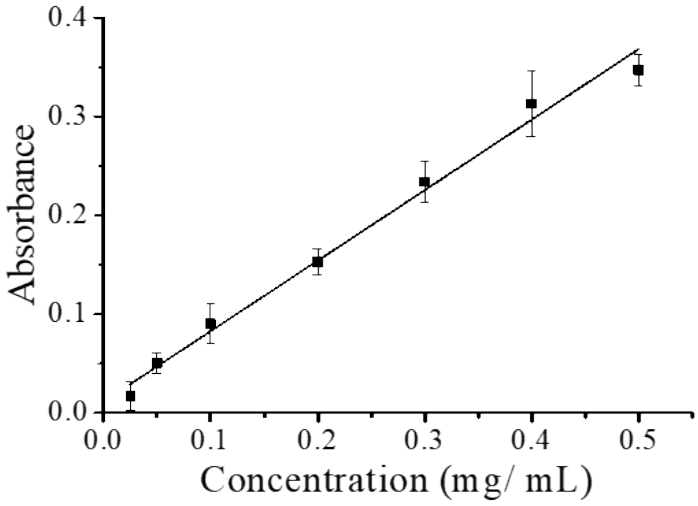

Figure. S6. Bicinchoninic acid (BCA) assays demonstrated the amount of GOx assembled on the Ru NFs.

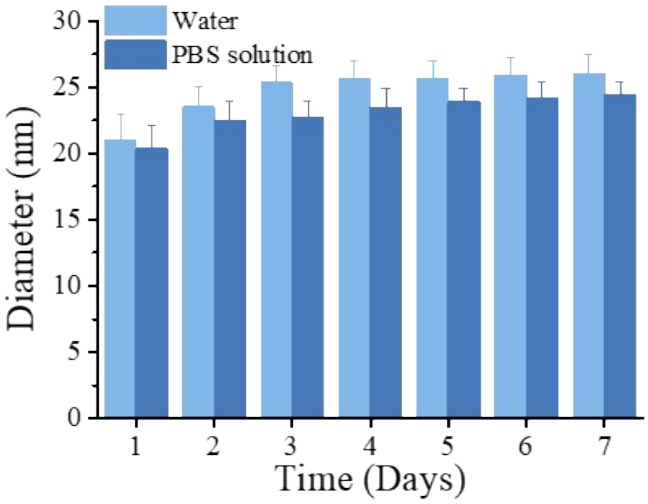

Figure. S7. Hydrodynamic diameter of HA-Ru NFs/GOx in aqueous and PBS solution during 7-day storage.

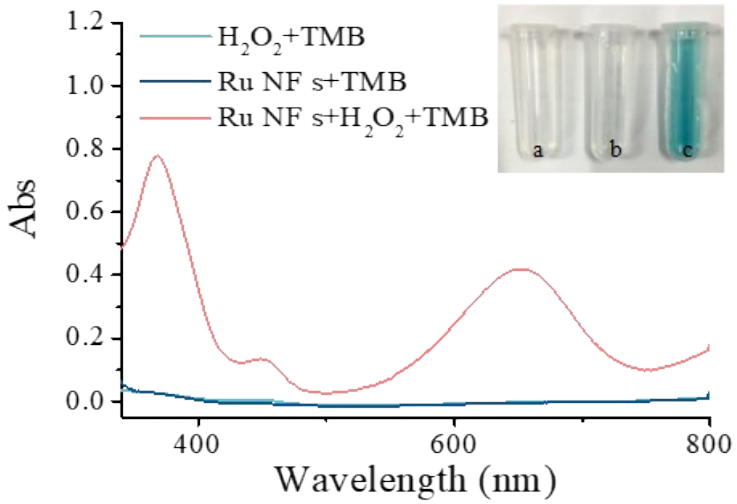

Figure. S8. UV−vis spectra of HA-Ru NFs/GOx with or without H_2O_2 in the presence of TMB.

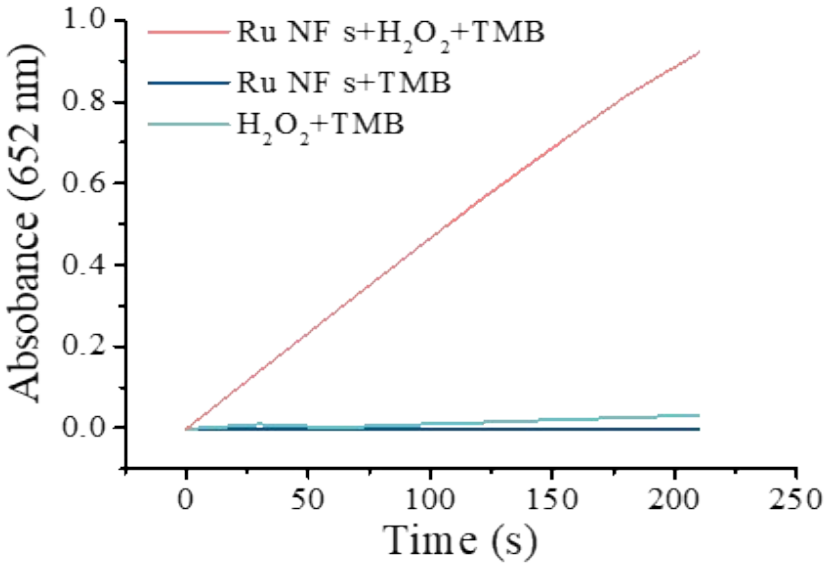

Figure. S9. Change in absorbance at 652 nm over time.

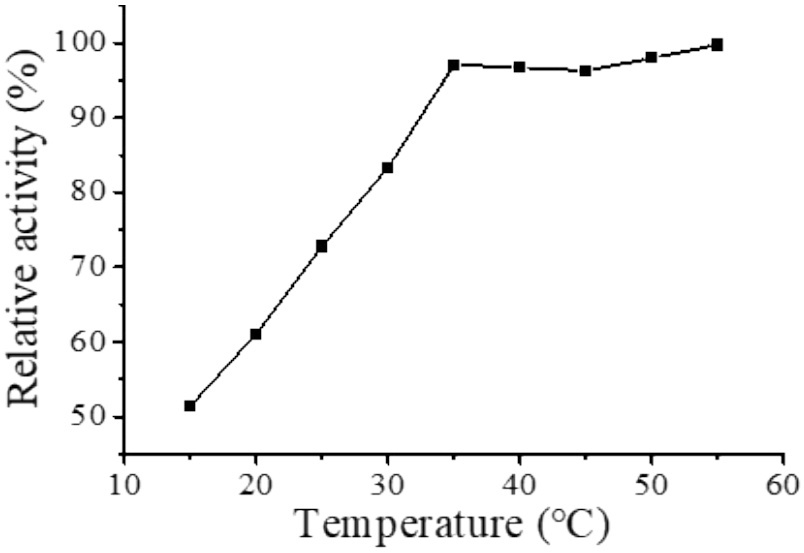

Figure. S10. Peroxidase-like activity of Ru NFs depending on temperature.

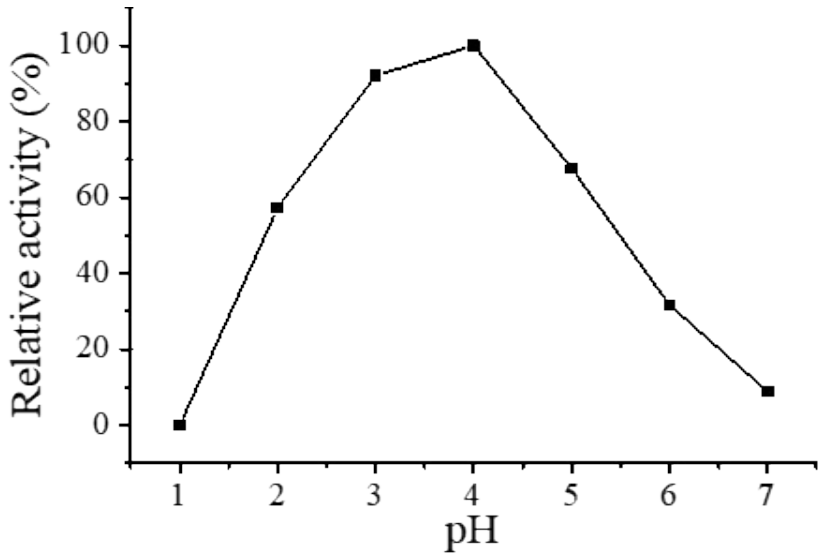

Figure. S11. Peroxidase-like activity of Ru NFs depending on pH value.

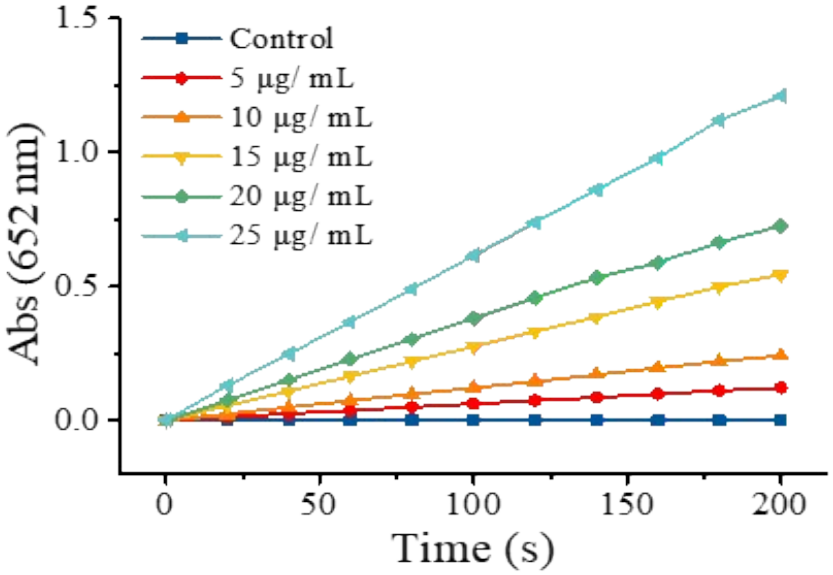

Figure. S12. Peroxidase-like activity of Ru NFs depending on Ru NFs concentration.

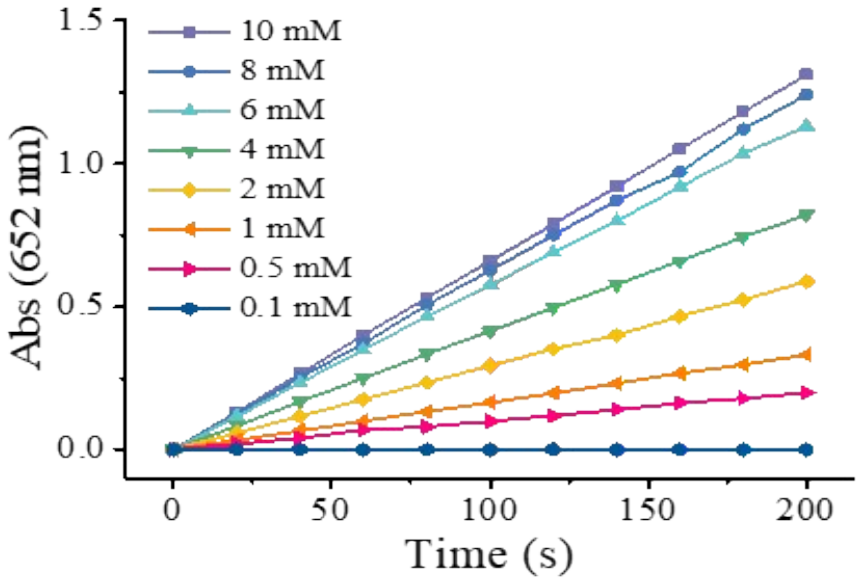

Figure. S13. Peroxidase-like activity of Ru NFs depending on H_2O_2 concentration.

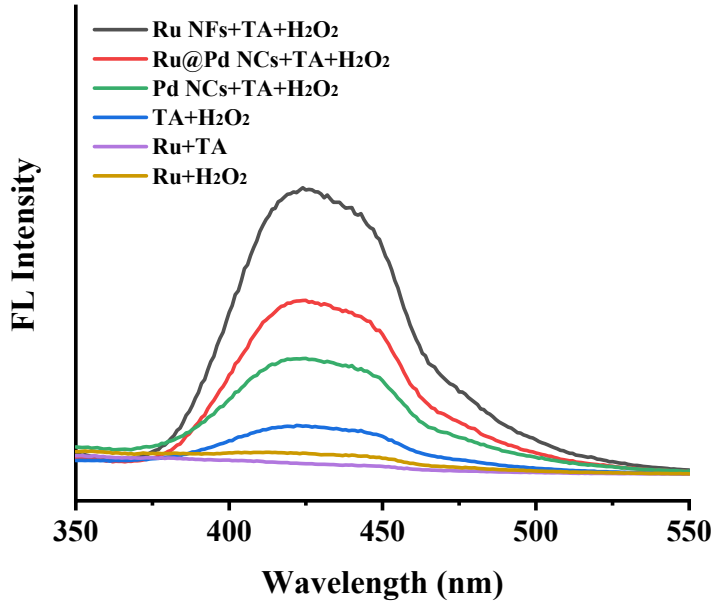

Figure. S14. Fluorescence spectra of different reaction systems: Ru NFs + TA + H_2O_2, Ru@Pd NCs + TA + H_2O_2, Pd NCs + TA + H_2O_2, TA + H_2O_2, Ru + TA and Ru + H_2O_2.

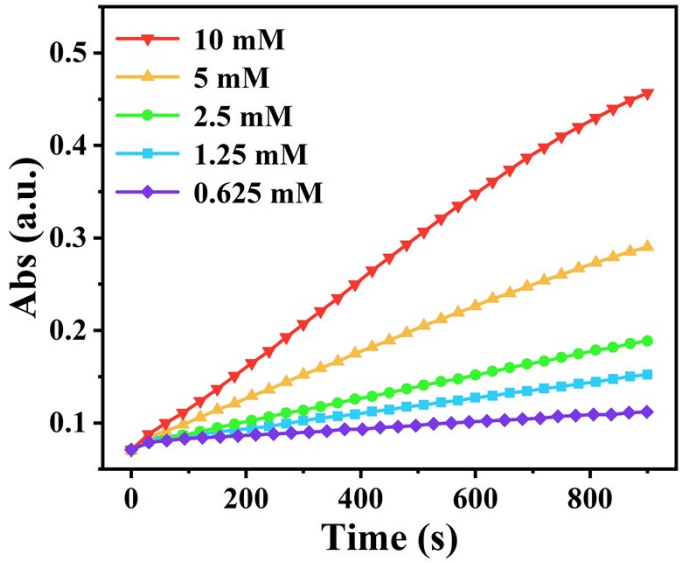

Figure. S15. Peroxidase-like activity of Ru NFs/GOx depending on H_2O_2 concentration.

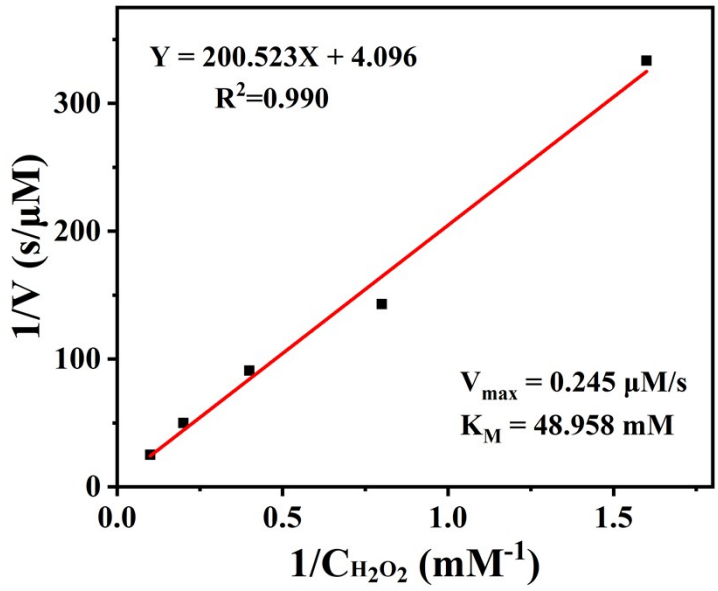

Figure. S16. Lineweaver–Burk plotting for Ru NFs/GOx with H_2O_2 as substrate. The steady-state catalytic rate (v) was calculated from the initial slopes of absorbance versus time plots in Figure. S14.

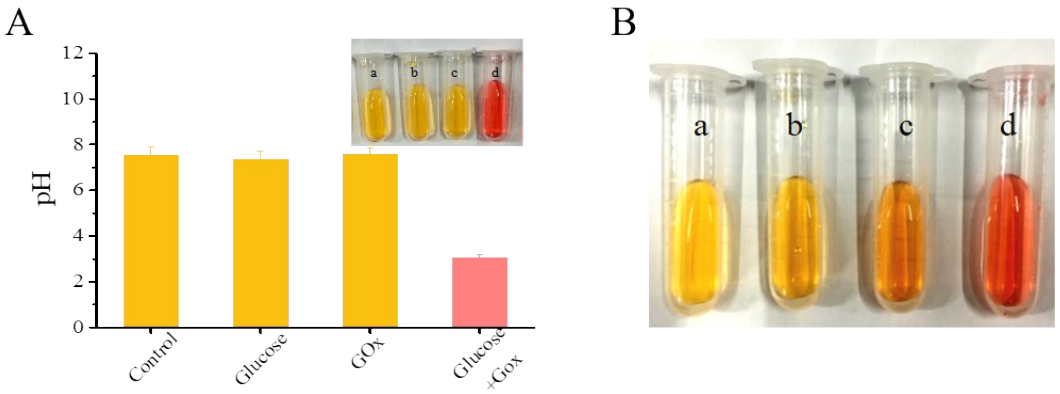

Figure. S17. (A) The pH value and photos of different reactions with the addition of methyl orange in PBS: (a) control, (b) only glucose, (c) only GOx, (d) glucose + GOx; (B) Photos of PBS at different pH values upon the addition of methyl orange: (a) pH=3, (b) pH=4, (c) pH=5, (d) pH=6.

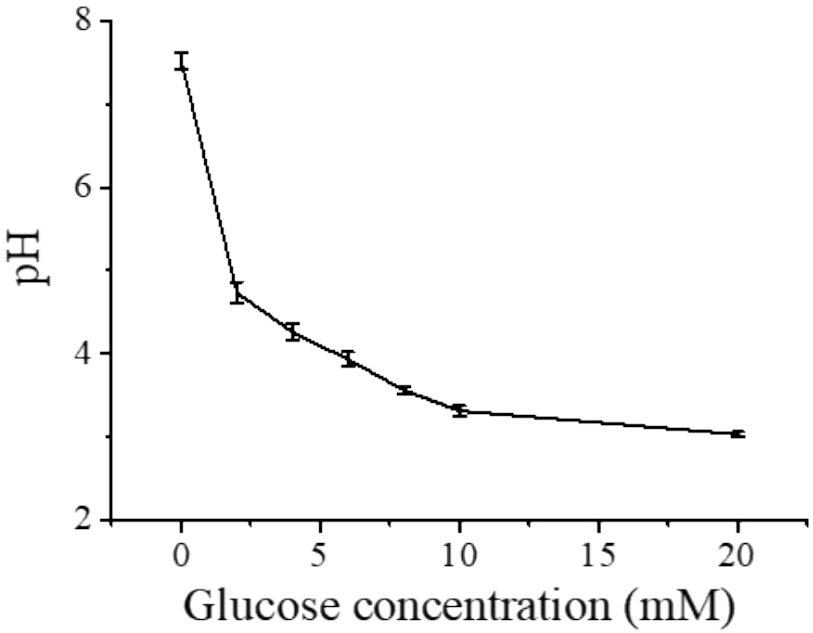

Figure. S18. Variation of pH value of reactions between GOx and different concentrations of glucose.

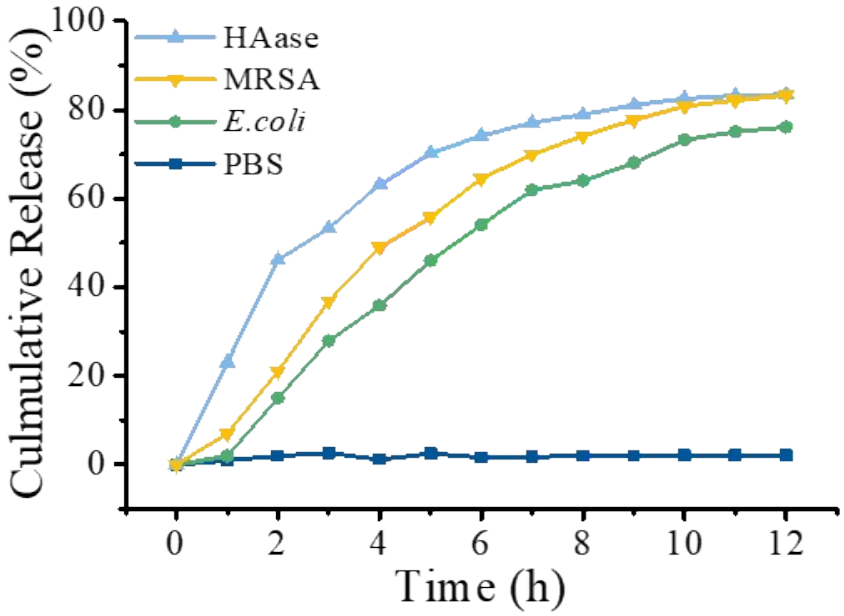

Figure. S19. Responsive release profile of HA-Ru NFs/GOx.

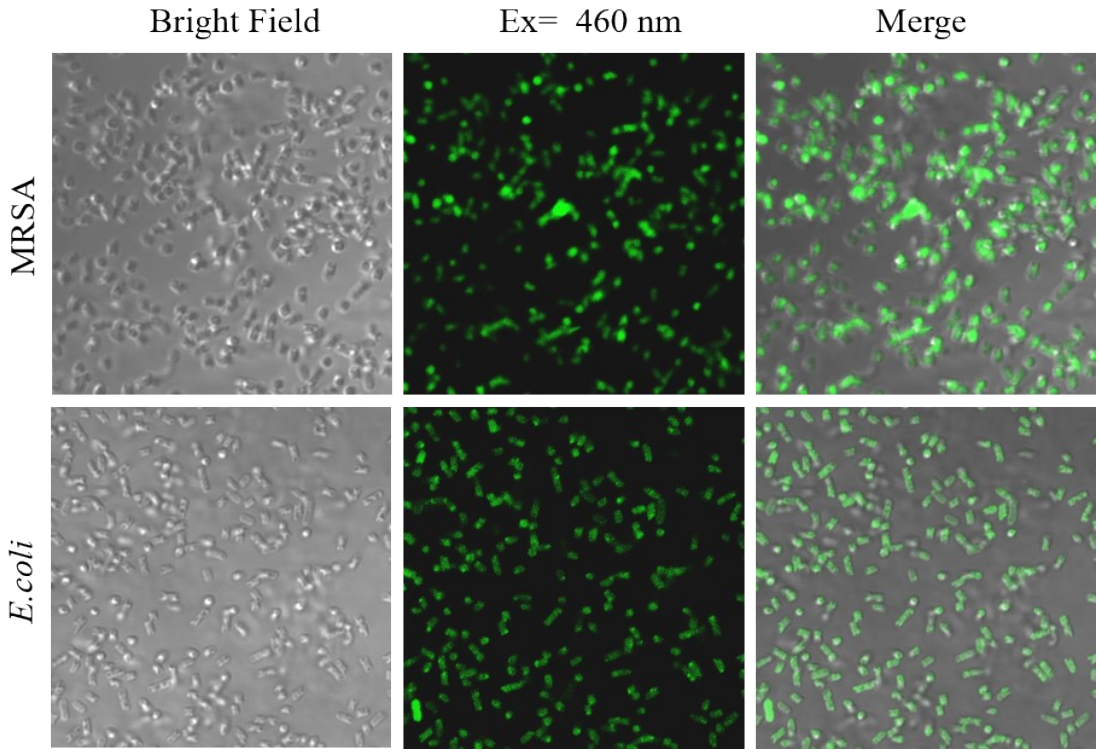

Figure. S20. Cellular total ROS probed with 2,7-dichlorofluorescein diacetate (DCFH-DA) detected with Laser scanning confocal microscope (MRSA and *E. coli*).

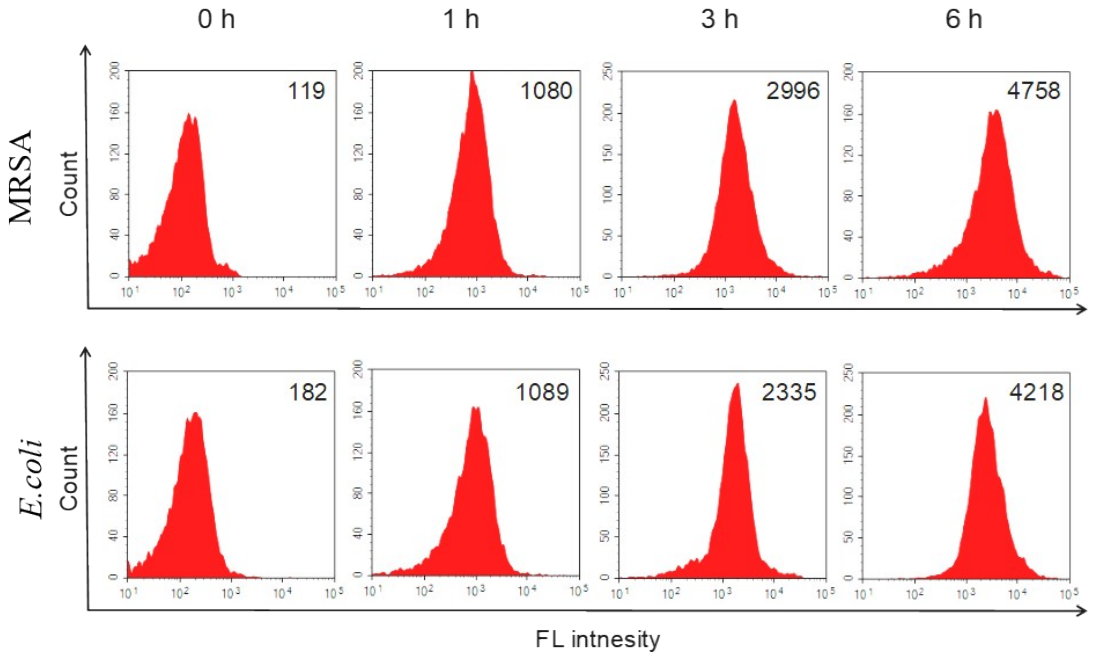

Figure. S21. Measurement of ROS level in the two kinds of bacteria, respectively, using flow cytometry after dying with DCFH-DA.

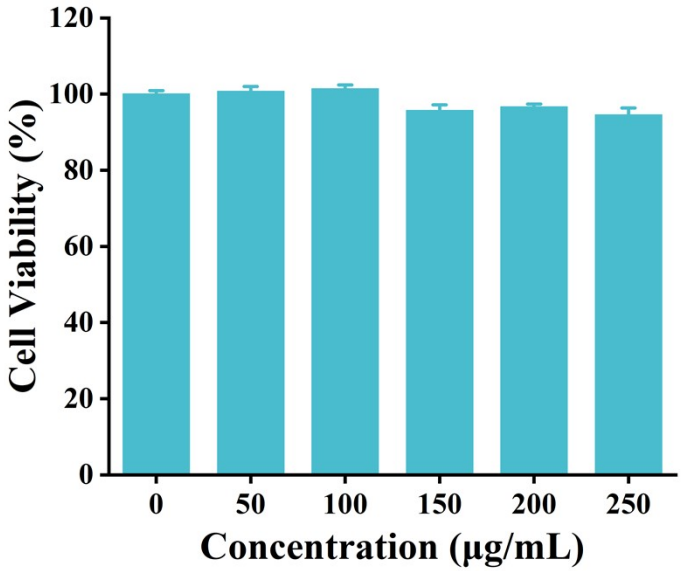

Figure. S22. Cell viability of HUVEC cells after treated with HA-Ru NFs/GOx at various concentrations for 24 h

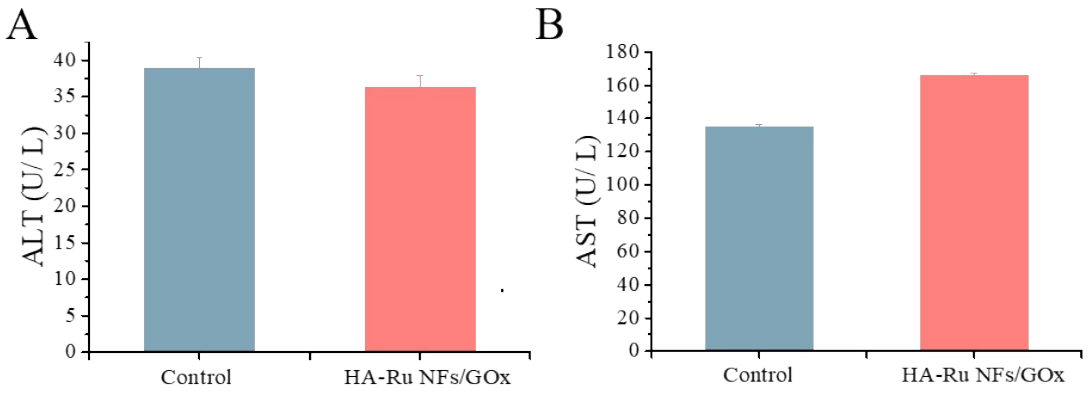

Figure. S23. (A) and (B) Comparison of ALT and AST levels in blood after treatment with glucose + HA-Ru NFs/GOx. Data were presented as mean ± s.d. (n= 3).